On-Wafer Electrooptic Probing Using Rotational Deformation Modulation

W. H. Chen, W. K. Kuo, S. L. Huang, *Member, IEEE*, and Y. T. Huang

***Abstract*—On-wafer electrooptic probing of two-dimensional electric-field vector (E-vector) is demonstrated by using one laser beam and one electrooptic prober. This technique utilizes both compressed-stretched deformation and rotational deformation on the index ellipsoid of the electrooptic crystal. Both experiment and simulation were performed to map the E-vector on a circuit board, and the measurement error is within 2.2%.**

***Index Terms*—Nondestructive testing, polarimetry.**

I. Introduction

ELECTROOPTIC (EO) probing techniques have beeen advancing very quickly in recent years [1]–[5] due to their superior features in characterization of semiconductor devices and circuits. These techniques allow the measurement of the electric field at any point on the device under test (DUT) [6]. Both analog and digital IC measurements are suitable for EO probing techniques [7], [8]. Some of the EO probing techniques are able to measure not only the electric-field amplitude, but also direction of the electric field [1], [2], [5]. Valuable information such as chamfered bending transmission lines and patch antennas of radio frequency devices can be released [5]. The conventional systems often require two beams or two different EO crystals to differentiate the directions of the electric field under test because only one type of EO modulation effect is utilized in the measurement. The measurements are, thus, inaccurate and complicated because the path length and EO interaction strength of the two probing beams are different [1], [5]. Now, we demonstrate the EO probing technique with one beam and one EO crystal to extract two–dimensional (2-D) electric-field vector (E-vector) using an additional modulation effect, i.e., rotational deformation modulation (RDM). In contrast to the conventional compressed/stretched deformation on the index ellipsoid of the EO crystal, RDM utilizes the rotation of principal axes. With the inclusion of this modulation technique, 2-D E-vector measurement is realized. The commercial software Ansoft Maxell 3-D Field Simulator is employed to verify our measurements. Good agreement is obtained between experiment and simulation results. This E-vector measurement technique is compact, accurate, and low cost.

Manuscript received February 1, 2000; revised May 1, 2000.

W. H. Chen and S. L. Huang are with the Institute of Electro-Optical Engineering, National Sun Yat-Sen University, Kaohsiung, Taiwan 804, R.O.C.

W. K. Kuo is with the Institute of Electronics, National Chiao-Tung University, Hsinchu, Taiwan 300, R.O.C., and also with the Precision Instrument Development Center, National Science Council, Hsinchu, Taiwan 300, R.O.C.

Y. T. Huang is with the Institute of Electronics, National Chiao-Tung University, Hsinchu, Taiwan 300, R.O.C.

Publisher Item Identifier S 1041-1135(00)07441-3.

II. System Description

A. Measurement Principle

1) Rotational Deformation Modulation: Depending upon the space group of EO crystals and the applied E-vector, the index ellipsoid of EO crystal experiences compressed/stretched deformation or rotational deformation. The compressed/stretched deformation has been applied in amplitude modulation for a long time [9], so we do not describe it in detail here. Not all EO crystals experience rotational deformation when the electric field is applied. Therefore, the EO crystal for RDM needs to be properly selected and biased.

Consider a beam incident on an electric biased EO crystal along its *z axis*. The cross-sectional ellipse of the index ellipsoid equation when cutting perpendicular to the propagation vector can be expressed as

$$\left(\frac{1}{n_x^2}+\alpha\right)x^2+\left(\frac{1}{n_y^2}+\beta\right)y^2+2\gamma xy=1 \tag{1}$$

where

$$\alpha = r_1 \cdot f(E_x, E_y, E_z)$$
$$\beta = r_2 \cdot f(E_x, E_y, E_z)$$
$$\gamma = r_3 \cdot f(E_x, E_y, E_z)$$

where n_x, n_y are the intrinsic indexes, and r_1, r_2 and r_3 are Pockels coefficients. $f(E_x, E_y, E_z)$ is a function of E_x, E_y and E_z. The rotation angle θ, of the principal axes can be obtained by analyzing (1). If the conditions of $n_x = n_y$ and $\alpha = \beta = 0$ both hold, the rotation angle is 45°. In general, the applied electric field is much smaller than the half-wave electric field required for typical EO crystals. Therefore, when n_x is not equal to n_y, θ can be estimated as

$$\theta \approx \frac{\gamma}{\dfrac{1}{n_x^2}-\dfrac{1}{n_y^2}+\alpha-\beta}. \tag{2}$$

When α, β are both zero or $\alpha-\beta$ is much smaller than $(1/n_x^2)-(1/n_y^2)$, θ is proportional to the electric field amplitude. An RDM system can, therefore, be constructed with this property as shown in Fig. 1. A polarizer and a Wollaston prism are used in this system. According to the analysis by using Jones matrix, the intensity of output beam, I_{RDM}, detected by the differential photodetector is

$$I_{\mathrm{RDM}} = -\sin^2(\delta)\sin(4\theta) \tag{3}$$

where δ is the phase retardation induced by the static birefringence of the EO crystal. For typical values of on-wafer electric

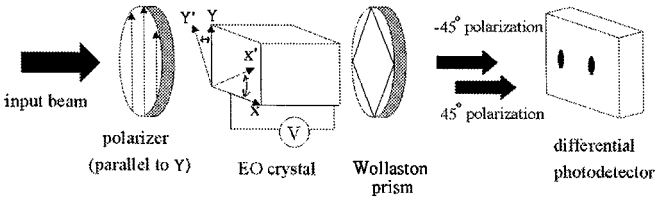

Fig. 1. The rotational deformation modulation system. As the electric field is applied on the EO crystal, the X and Y axes of index ellipsoid rotate to X' and Y', respectively.

field, 4θ is much smaller than 1. Therefore, $\sin(4\theta)$ can be approximated as 4θ and I_{RDM} becomes proportional to θ. This system can, therefore, modulate the input beam linearly. The quarter-wave plate usually used for compressed/stretched deformation modulation (CSDM) system is no longer needed [9], because RDM can work without a retardation bias.

Based on the above discussion, a cubic crystal is not suitable for RDM because its $n_x = n_y$ and $\alpha = \beta = 0$, while EO crystals of $\overline{4}2m$ and $3m$ space groups are good for RDM. $LiTaO_3$ is selected as the EO crystal in our experimental system not only because it is suitable to RDM, but it also has a good compressed/stretched deformation effect. Moreover, its rotational deformation and compressed/stretched deformation are induced by the electric field of different directions.

2) The Principle of 2-D E-Vector Measurement: The EO tensor of $LiTaO_3$ can be expressed as

$$[r_{ij}] = \begin{bmatrix} 0 & -r_{22} & r_{13} \\ 0 & r_{22} & r_{13} \\ 0 & 0 & r_{33} \\ 0 & r_{51} & 0 \\ r_{51} & 0 & 0 \\ -r_{22} & 0 & 0 \end{bmatrix}. \tag{4}$$

At the wavelength of 633 nm, n_o and n_e of $LiTaO_3$ are 2.176 and 2.180, respectively, and the EO coefficients, r_{13}, r_{33}, r_{22}, and r_{51} are 8.4×10^{-12}, 30.5×10^{-12}, -0.2×10^{-12}, and 22×10^{-12} m/V, respectively.

By analyzing the index-ellipsoid deformation of $LiTaO_3$ under electric-field bias in our propagation path, as shown in Fig. 2(a), it can be proved that E_y has no RDM effect. Moreover, the E_y effect on CSDM in our experiment is negligible according to a previous study [1]. The rotation angle for the principal axes of the index ellipsoid $\theta(E_x)$ is proportional to E_x, and the phase retardation $\delta(E_z)$ caused by the EO effect of $LiTaO_3$ is proportional to E_z. RDM and CSDM are caused by E_x and E_z, respectively, in our probing system, as shown in Fig. 2(b). According to the calculation of Jones matrix, the intensity of detected light, Iin our experimental setup is

$$I = A\cos(2\phi) \cdot \theta(E_x) + B\sin(2\phi) \cdot \delta(E_z) \tag{5}$$

where A and B are constants, and ϕ is the polarization angle of the incident beam with respect to the z axis as shown in Fig. 2(c). The modulation type corresponds to the polarization of incident beam. When ϕ is 0°, i.e., the polarization is along the z axis, (5) becomes

$$I_{0^\circ} = A \cdot \theta(E_x) = A_1 \cdot E_x \tag{6}$$

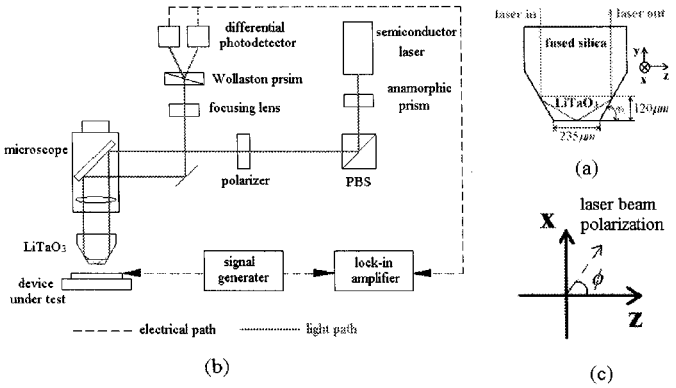

Fig. 2. (a) The propagation path of the incident beam in the $LiTaO_3$. (b) The on-wafer EO probing system using RDM and CSDM. (c) The polarization angle of incident beam. z is the optic axis of $LiTaO_3$.

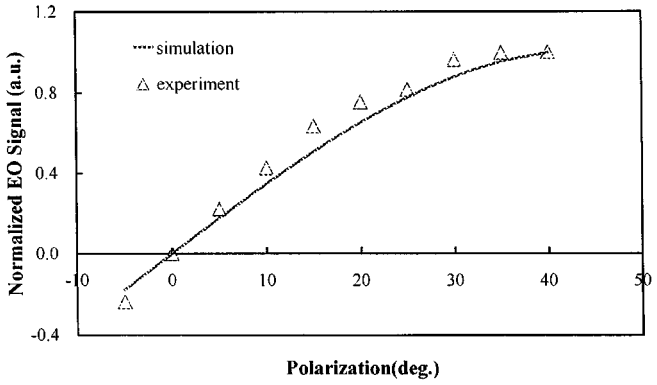

Fig. 3. The EO signal response corresponds to different polarizations.

where A_1 is a constant; the intensity of detected light I_{0° is proportional to E_x, and only RDM exists. When ϕ is 45°, the intensity of detected light becomes

$$I_{45^\circ} = B \cdot \delta(E_z) = B_1 \cdot E_z \tag{7}$$

where B_1 is a constant; I_{45°, is proportional to E_z, and only CSDM exists.

The A_1 to B_1 ratio can be determined with high accuracy with the same beam. Therefore, the E-vectors can be obtained by utilizing two different polarizations.

B. Experimental Setup

The experimental system is shown in Fig. 2(b). A single-longitudinal-mode laser diode is used as the light source (wavelength = 635 nm), which is followed by a 3-to-1 anamorphic prism to complete its divergent angle in vertical and horizontal directions. $LiTaO_3$ is employed as the EO crystal. The beam path in the $LiTaO_3$ crystal is shown in Fig. 2(a). The beam propagates in the y-z plane. A polarizer is placed in front of the EO crystal to control the polarization of the incident beam. Low-noise photodetection is achieved by using a differential photodetector and a lock-in amplifier. A 1-kHz square-wave signal is fed to the device as the test signal.

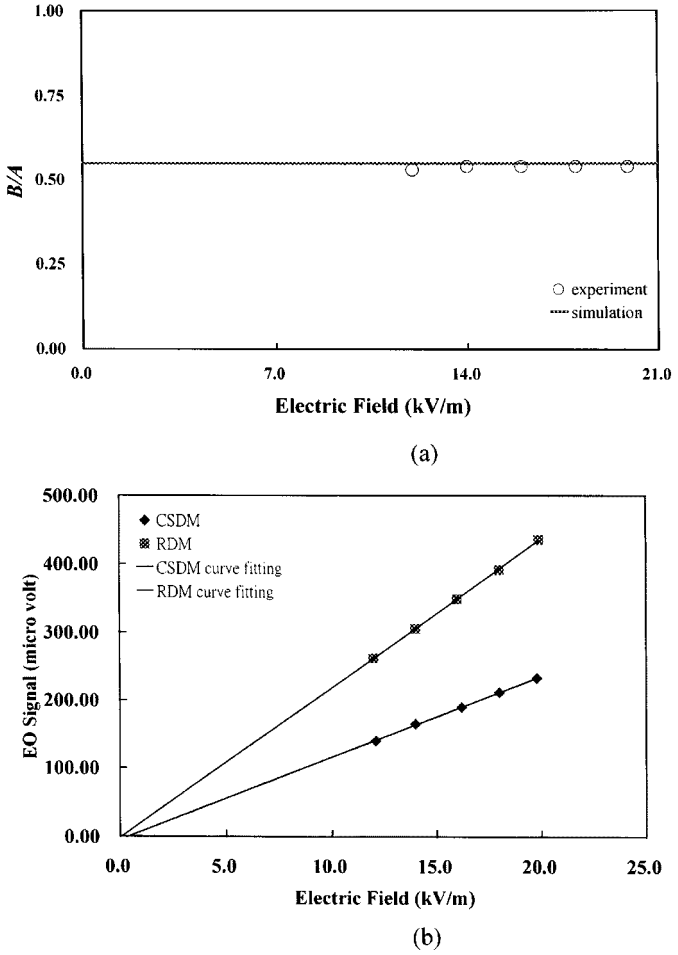

Fig. 4. (a) The simulation and experimental results of B to A ratios. (b) Using RDM and CSDM to measure the E_x and E_z.

III. Experimental Results

Several experiments were performed to demonstrate the one-beam EO probing technique for mapping a 2-D E-vector. First, we applied E_z onto the DUT to measure the EO signal response for different polarizations, as shown in Fig. 3. When the beam polarization was 0°, no EO signal was detected because of no relative phase retardation. This agrees with (5) well. Secondly, constants A and B of (5) were determined by varying the applied electric-field strength. Fig. 4(a) shows that the B to A ratio agrees well with our simulation results. The average error of this experimental result is 2.2% and the standard deviation is 0.8%. All of these results prove that the RDM technique is feasible. Fig. 4(b) shows the measurement results of RDM and CSDM, respectively. The RDM and CSDM curves both have a linear relationship to the electric field, as expected. This means CSDM and RDM both can work successfully in our experimental system.

The final experiment is a 2-D E-vector measurement of the DUT shown in Fig. 5. The DUT is an unsymmetrical metal gap, which is made on a dielectric substrate. The gap width is 0.5 mm. The measured electric field along "route 1" and "route 2" on the DUT are in good agreement with the simulation by the commercial software Ansoft Maxell 3-D Field Simulator. The E_z simulation curve along "route 1" is a little incongruous near

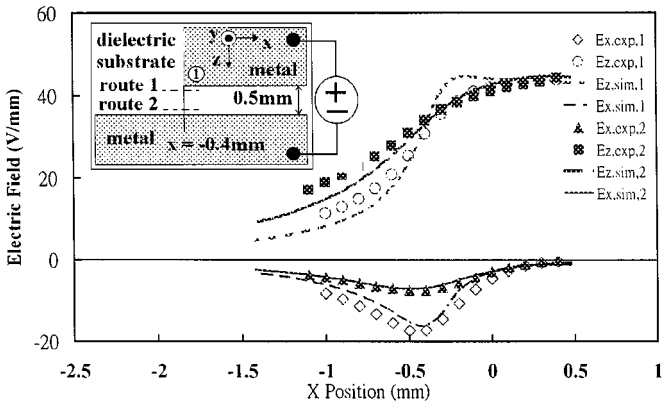

Fig. 5. The inset at the upper left corner is DUT, and "route 1" and "route 2" are the measurement paths. The marks are 2-D electric field measurement results, and the curves are simulation results. The subscripts "1" and "2" represent the data obtained from route 1 and route 2, respectively.

corner ○1, because the curvature of corner ○1 was difficult to estimate accurately.

IV. Conclusion

On-wafer EO probing using rotational deformation modulation has been demonstrated successfully. This new probing technique not only simplifies the conventional measurement processes and systems, it also improves measurement accuracy. Therefore, a low-cost approach for E-vector measurement can be achieved. The RDM technique can also be applied to 3-D E-vector measurement with only two beams.

Acknowledgment

The authors would like to thank the National Center for High-Performance Computing, National Science Council, Taiwan, R.O.C., for the use of simulation hardware and software. We also thank Dr. H. Z. Cheng for her enthusiastic assistance and support.

References

[1] W. K. Kuo, S. L. Huang, T. S. Horng, and L. C. Chang, "Two-dimensional mapping of electric-field vector by electro-optic prober," *Opt. Commun.*, vol. 149, pp. 55–60, 1998.

[2] W. K. Kuo, Y. T. Huang, and S. L. Huang, "Three- dimensional electric-field vector measurement with an electro-optic sensing technique," *Opt. Lett.*, vol. 24, pp. 1546–1548, 1999.

[3] H. Takahashi, S. Aoshima, and Y. Tsuchiya, "Sampling and real-time methods in electro-optic probing system," *IEEE Trans. Instrum. Meas.*, vol. 44, pp. 965–971, Oct. 1995.

[4] D. L. Quang, D. Erasme, and B. Huyart, "MMIC-calibrated probing by CW electrooptic modulation," *IEEE Trans. Microwave Theory Tech.*, vol. 43, pp. 1031–1036, May 1995.

[5] K. Kamogawa, I. Toyoda, K. Nishikawa, and T. Tokumitsu, "Characterization of a monolithic slot antenna using an electro-optic sampling technique," *IEEE Microwave Guided Wave Lett.*, vol. 4, pp. 414–416, Dec. 1994.

[6] J. A. Valdmanis and G. Mourou, "Subpicosecond electrooptic sampling: Principles and applications," *IEEE J. Quantum Electron.*, vol. QE-22, pp. 69–78, Jan. 1986.

[7] M. Shinagawa and T. Nagatsuma, "A laser-diode-based picosecond electrooptic prober for high-speed LSI's," *IEEE Trans. Instrum. Meas.*, vol. 41, pp. 375–380, June 1992.

[8] G. David, T. Y. Yun, M. H. Crites, J. F. Whitaker, T. R. Weatherford, K. Jobe, S. Meyer, M. J. Bustamante, B. Goyette, S. Thomas III, and K. R. Elliott, "Absolute potential measurements inside microwave digital IC's using a micromachined photoconductive sampling probe," *IEEE Trans. Microwave Theory Tech.*, vol. 46, pp. 2330–2337, Dec. 1998.

[9] A. Yariv, *Optical Electronics in Modern Communications*. Oxford, U.K.: Oxford Univ. Press, 1997, ch. 9.